has also been reported for $(COT)Os(CO)_3$.[43] It is in the cobalt subgroup that evidence for either 1,5- or 1,3-coordination of η^4-COT occurs, for the same metal, not only in the present work but also previously in that of Smith and Maitlas,[43] who were able to isolate $(1,3\text{-}COT)MC_5Me_5$ (M = Rh, Ir) from low-temperature reactions of COT^{2-} with $[M(C_5Me_5)Cl_2]_2$. The 1,3-isomers irreversibly arranged to $(1,5\text{-}COT)MC_5Me_5$ upon warming to room temperature.

Thus, it is apparent that sometimes subtle changes in electronic requirement may have a significant effect on the structural preferences of cyclooctapolyene ligands. The most important contributions of our presently reported work is the discovery that changes in isomeric preferences may accompany changes in electron count (or, if you wish, formal metal oxidation state) of these complexes. This raises the possibility of *control* of isomeric structure through redox chemistry of the organometallic π complex.

The compounds reported in the previous literature, discussed above,[34-43] are all 18-electron species. The isomerizations of $(1,5\text{-}COT)CoCp^-$ and $(1,5\text{-}COD)CoCp^-$ (both 19-electron species) represent the first data on structural preferences of C_8 polyene rings for organometallic *radical ions*. Many questions are raised by these observations, especially concerning the role of the metal in the isomerizations and how the electronic structure[44] of the anions (charge localization, radical character) affects the processes. A further, important, consideration is whether or not this phenomenon of redox-initiated isomerization of nonconjugated to conjugated hydrocarbons will be found to be general for other, smaller or larger, polyolefin rings. These questions are currently under study.

Acknowledgment. We gratefully acknowledge support by the National Science Foundation of this work, and we thank John L. Spencer for his gift of $(COT)CoC_5Me_5$.

(43) Smith, A. K.; Maitlis, P. M. *J. Chem. Soc., Dalton Trans.* **1976**, 1773–1777.

(44) For electron spin resonance data and results of molecular orbital calculations on these compounds, see: Albright, T. A.; Geiger, W. E.; Moraczewski, J.; Tulyathan, B. *J. Am. Chem. Soc.*, following paper in this issue.

Structural Consequences of Electron-Transfer Reactions. 6.[1] Electronic Structures and Structural Preferences of Cyclooctatetraene and Cyclooctadiene Iron and Cobalt Compounds and Their Radical Anions

Thomas A. Albright,*[2a,c] William E. Geiger, Jr.,*[2b] Jerry Moraczewski,[2b] and Bunchai Tulyathan[2b]

Contribution from the Departments of Chemistry, University of Houston, Houston, Texas 77004, and University of Vermont, Burlington, Vermont 05405. *Received December 1, 1980*

Abstract: ESR spectra of (1,3-cyclooctatetraene)$CoCp^-$, $-Fe(CO)_3^-$, and $-Fe(CO)_2(PPh_3)^-$ were obtained. It is shown by the magnitude of the hyperfine couplings for $(1,3\text{-}COT)CoCp^-$ that the odd electron resides in the COT portion of the molecule. Strong evidence for an analogous situation in the Fe complexes is also presented. On the other hand, the ESR spectra for (1,5-cyclooctadiene)$CoCp^-$ and the 1,3-isomer show that the unpaired electron in both cases is predominately metal centered. These findings are corroborated by molecular orbital calculations of the extended Hückel type. Along with a description of the nature of the singly occupied orbital in these reduced species, details of the geometric structure are presented. The relative ease of reduction and pathways interconverting the 1,3- and 1,5-isomers of (COT)CoCp are also given.

Cyclooctatetraene (COT) and cyclooctadiene (COD) are common ligands in organometallic chemistry. Much of their chemistry has been investigated with an emphasis on the mode of coordination to the transition-metal and the fluxional properties of some of the compounds.[3] Complexes of COT from η^8 to η^2 are known. This engenders a variety of geometries that the COT ligand can adopt. An elegant description of this has been given by Guggenberger and Schrock.[4] COT itself is tub-shaped.[5] Reduction to the dianion flattens the ring[6] to D_{8h} symmetry in accord with the prediction by Hückel's rule. One of the more interesting observations made is that even when an 8-membered ring (e.g., COT or COD) is restricted by the 18-electron rule to η^4 coordination, the ligand may bond either as a chelating 1,5-diene (η^4-1,2,5,6 bonding, through nonadjacent double bonds) or as a conjugated 1,3-diene (η^4-1,2,3,4 bonding). The electronic factors which govern the favored mode of bonding are not known. We have recently discovered that the total number of electrons possessed by the metal π complex can have a determining effect on whether the 1,5- or 1,3-bonded isomer is favored.[1,7] In particular, half-occupancy of the lowest unoccupied molecular orbital (LUMO) of (COT)CoCp or (COD)CoCp (Cp = η^5-C_5H_5) by one-electron reduction of the neutral compounds facilitates conversion of the 1,5-isomer to the 1,3-isomer. Obviously, the

(1) Part 5: Moraczewski, J.; Geiger, W. E., Jr. *J. Am. Chem. Soc.*, preceding paper in this issue.

(2) (a) University of Houston. (b) University of Vermont. (c) Camille and Henry Dreyfus Teacher-Scholar, 1979–1984.

(3) For reviews see: Bennett, M. A. *Adv. Organomet. Chem.* **1966**, *4*, 353. Deganello, G. "Transition Metal Complexes of Cyclic Polyolefins"; Academic Press: New York, 1979: Chapter 2.

(4) Guggenberger, L. J.; Schrock, R. R. *J. Am. Chem. Soc.* **1975**, *97*, 6693.

(5) (a) Traetteberg, M. *Acta. Chem. Scand.* **1966**, *20*, 1724. (b) Bordner, J.; Parker, R. G.; Stanford, R. H., Jr. *Acta Crystallogr., Sect. B.* **1972**, *B28*, 1069. (c) Davis, R., private communication on C_8F_8. (d) Wheatley, P. J. *J. Chem. Soc.* **1965**, 3136. (e) Pawley, G. S.; Lipscomb, W. N.; Freedman, H. H. *J. Am. Chem. Soc.* **1964**, *86*, 4725. (f) Shoemaker, D. P.; Kindler, H.; Sly, W. G.; Srivastave, R. C. *Ibid.* **1965**, *87*, 482. (g) Avitabile, G.; Ganis, P.; Petraccone, V. *J. Phys. Chem.* **1969**, *73*, 2378. (h) Wright, D. A.; Seff, K.; Shoemaker, D. P. *J. Cryst. Mol. Struct.* **1972**, *2*, 41.

(6) Goldberg, S. Z.; Raymond, K. N.; Harmon, C. A.; Templeton, D. H. *J. Am. Chem. Soc.* **1974**, *96*, 1348.

(7) Moraczewski, J.; Geiger, W. E., Jr. *J. Am. Chem. Soc.* **1979**, *101*, 3407.

0002-7863/81/1503-4787$01.25/0

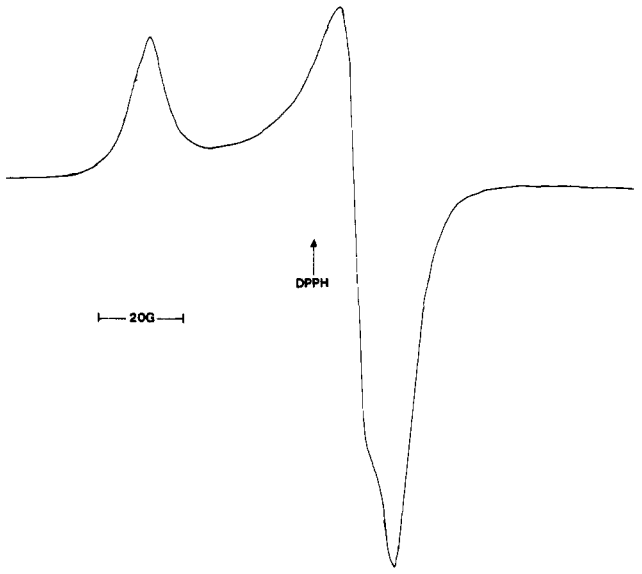

Figure 1. ESR spectrum of frozen solution of (1,3-COT)Fe(CO)$_3^-$ in DMF at 163 K. Solution was produced by electrolytic reduction of a 1.0 × 10^{-3} M solution of (COT)Fe(CO)$_3$ in DMF/0.1 M Bu_4NPF_6 at a mercury pool at −1.5 V under N_2.

electronic structures of these compounds and their radical ions are important in determining the mode of polyolefin bonding. This paper investigates those electronic structures through calculations of the extended-Hückel type[8] and electron spin resonance measurements of their radical anions. The compounds investigated were (1,5-COT)CoCp (**1**), (1,3-COT)CoCp (**2**), (1,3-COT)Fe(CO)$_3$ (**3**), (1,5-COD)CoCp (**4**), and (1,3-COD)CoCp (**5**).

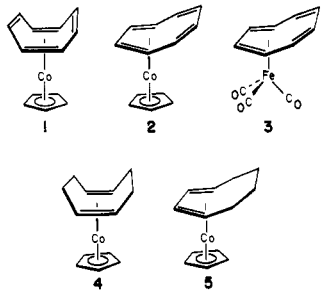

Experimental Section

All electron spin resonance spectra were obtained by a Varian X-band Model V4500-10A spectrometer with a 100-kHz field modulation and 9-in. magnet. The temperature of the probe was controlled through use of the Model V-4540 variable-temperature controller. For measurement of g values, a dual cavity was employed with diphenylpicrylhydrazyl (DPPH) as the reference standard (g = 2.0036). We have previously described the methods for the preparation of these compounds, solvents, and electrochemical procedures.[1] (1,3-COT)Fe(CO)$_2$(PPh$_3$) was generously supplied by Dr. Neil Connelly of the University of Bristol. Chemical reductions were performed by using Na/K alloy (MSA Research Corp.) in a two-compartment cell under high vacuum. Working under nitrogen, the alloy was loaded into one compartment and a few milligrams of the compound loaded into the other chamber. After evacuation of the vessel to a minimum vacuum of 10^{-4} mmHg, tetrahydrofuran was bulb-to-bulb distilled into the sample chamber and the vessel was flame sealed. The THF solution containing the compound to be reduced was tipped into the alloy compartment to allow reduction to occur. Usually in a few seconds (at lower temperatures, in several minutes) a color change occurred. At this point the reduced solution was tipped into a 3-mm quartz ESR tube attached to the side of the vessel and the solution was quick-frozen by rapid immersion in liquid nitrogen. The frozen samples were then put into the low-temperature sample probe in the ESR cavity. Some spectra were also obtained by using sodium naphthalenide as reductant. In this case a sodium naphthalenide solution was substituted for the Na/K alloy in the two-compartment cell and a similar procedure was followed.

Esr spectra of the following radical anions were generated by electrochemical reductions at the potential of the first cathodic wave: (1,3-COT)Fe(CO)$_3^-$; (1,3-COT)Fe(CO)$_2$(PPh$_3$)$^-$; (1,3-COT)CoCp$^-$; (1,5-COD)CoCp$^-$ (in DMF); (1,3-COD)CoCp$^-$ (in THF). Na/K or sodium naphthalenide reduction could also be used to obtain spectra of (1,3-COT)CoCp$^-$ or (1,3-COD)CoCp$^-$.

Electron Spin Resonance Spectra

(1,3-COT)Fe(CO)$_3^-$ and (1,3-COT)Fe(CO)$_2$(PPh$_3$)$^-$. Stable (under N_2) solutions of these two iron anions were prepared by electrolysis at a mercury pool, at the potential of their first reduction waves[9-11] in DMF/0.1 M Bu_4NPF_6. Spectra at 150 K of the frozen solutions revealed a rhombic **g** tensor, with no apparent hyperfine splittings, even for the phosphine-containing radical. Figure 1 shows the ESR spectrum of (1,3-COT)Fe(CO)$_3^-$. Iron splittings are seldom seen in ESR spectroscopy because of the low natural abundance (2.19%) and small magnetogyric ratio of ^{57}Fe. Therefore, conclusions about the electronic structures of the iron anion radicals must be confined to qualitative arguments on the basis of the absence of hyperfine splittings and on the g values observed. The latter—see Table I—differ only slightly from the free-spin value of $g \approx 2$, and the degree of anisotropy is small ($g_1 - g_3 = 0.036$), indicating the virtual quenching of orbital angular momentum in the radical. This suggests strongly that the half-filled orbital resides predominantly on the ligand(s) rather than on the metal. Furthermore, the absence of ^{31}P splittings in (1,3-COT)Fe(CO)$_2$(PPh$_3$)$^-$ leads to the conclusion that the half-filled orbital in the anions resides *predominantly on the cyclooctatetraene portion* of the molecule.

To underscore this conclusion, contrast this data to that reported by Anderson and Symons,[12] who irradiated frozen matrices containing (η^4-cyclohexadiene)iron dicarbonyl triphenylphosphine and assigned the resulting spectra to the radical anion. These authors reported a rhombic **g** tensor with considerably higher anisotropy (g_1 = 2.075, g_2 = 2.062, g_3 = 2.006; $g_1 - g_3 = 0.069$) and a large ^{31}P splitting of axial symmetry ($a_1 = a_2$ = 55 G, a_3 = 68 G). Arguments were presented favoring a ground-state predominantly metal in character.

(1,3-COT)CoCp$^-$. Radical anions derived from cobalt π complexes have not been widely reported. In the examples that have been found[13-15] the powder or glassy spectra are characterized by an axially symmetric cobalt hyperfine tensor, with the unique (largest) splitting along the low-field direction. Typically, values of $a_\parallel$ = 100G to 150 G and $a_\perp$ ca. 40 G have been observed. Our frozen solution spectrum of (1,3-COT)CoCp$^-$, see Figure 2, is strikingly different than these spectra. The radical was best prepared by electrolysis of (COT)CoCp at a Hg pool at −2.1 V in THF/0.1 M Bu_4NPF_6. During the course of the electrolysis the solution changes from light yellow to dark orange, and CV scans showed that the mixture of 1,5- and 1,3-isomers of the neutral compound[1,7] had been converted exclusively to the anion of the 1,3-isomer. Samples were syringed out under N_2 and frozen for ESR analysis. The radical could also be obtained by sodium naphthalenide reduction, but poorer signal/noise spectra were obtained.

The spectrum of Figure 2 may be interpreted in terms of a rhombic **g** tensor in which the Co hyperfine splitting is *nearly*

(8) Hoffmann, R. *J. Chem. Phys.* **1963**, *39*, 1397. Hoffmann, R.; Lipscomb, W. N. *Ibid.* **1962**, *36*, 3179; **1962**, *37*, 2872.

(9) El Murr, N.; Riveccie, M.; Laviron, E. *Tetrahedron Lett.* **1976**, 3339.

(10) Tulyathan, B.; Geiger, W. E., Jr. *J. Electroanal. Chem.* **1980** *109*, 325.

(11) Electrochemical data on (1,3-COT)Fe(CO)$_2$(PPh$_3$) have not previously appeared. In DMF/0.1 M Bu_4NPF_6 at a hanging mercury drop electrode we find two waves, $E^\circ_1 = -1.62$ V, $E^\circ_2 = -1.87$ V, fully reversible by cyclic voltammetry.

(12) Anderson, O. P.; Symons, M. C. R. *Inorg. Chem.* **1973**, *12*, 1932.

(13) Van Willigen, H.; Geiger, W. E., Jr.; Rausch, M. D. *Inorg. Chem.* **1977**, *16*, 581.

(14) Elschenbroich, Ch., personal communication, 1979, University of Marburg.

(15) Geiger, W. E., Jr., unpublished ESR observations on anion radicals of quinone-CoCp compounds.

Table I. Electron Spin Resonance Parameters for (Cyclooctatetraene)- and (Cyclooctadiene)metal Anion Radicals

compd	matrix	a_1(Co), G	a_2(Co), G	a_3(Co), G	g_1	g_2	g_3
(1,3-COT)Fe(CO)$_3^-$ (3^-)	DMF, 163 K				2.016	2.009	1.980
(1,3-COT)Fe(Co)$_2$(PPh$_3$)$^-$	DMF, 163 K				2.014	2.009	1.979
(1,3-COT)CoCp$^-$ (2^-)	THF, 153 K	46	41[a]	41 G	2.196	2.022[a]	1.946
(1,5-COD)CoCp$^-$ (4^-)	DMF, 163 K	158	ca. 50		2.165	ca. 2.0	
(1,3-COD)CoCp$^-$ (5^-)	THF, 153 K	140	ca. 42		2.189	ca. 2.0	

[a] Estimated value. See text.

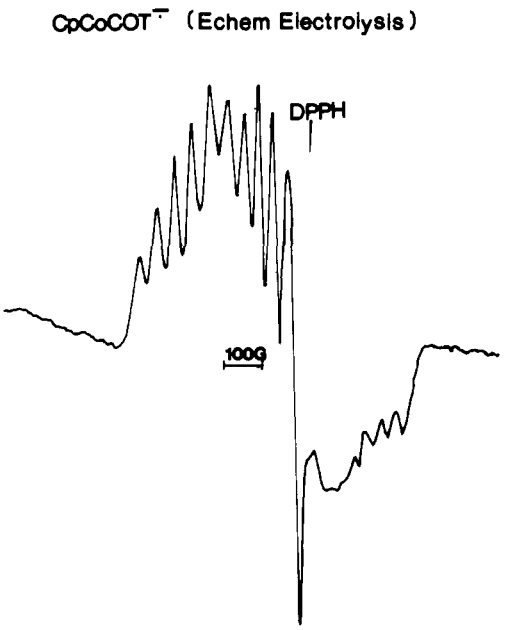

Figure 2. ESR spectrum of frozen solution of (1,3-COT)CoCp$^-$ in THF at 153 K. Solution was produced by electrolytic reduction of a 6.0×10^{-4} M solution of (COT)CoCp in THF/0.1 M Bu_4NPF_6 at a mercury pool at −2.2 V under N_2.

isotropic. If all cobalt hyperfine lines were resolved, a total of 24 lines would appear, due to the three octets (^{59}Co, 100%, $I = {}^7/_2$) for cobalt, one for each of the 3 principal directions of the **g** tensor. At least 6 of the 8 lines of the low-field multiplet are observed, with a_1 = 46 G. Similarly, at least 4 lines of the high-field multiplet are resolved, with A_3 = 41 G. Thus, we can measure accurately a_1, a_3, g_1, and g_3 (Table I). The overlapped middle part of the spectrum did not allow accurate determination of a_2 and g_2,[16,17] but a reasonable estimate of these values could be obtained. To obtain these, we measured the points at which the low- or high-field hyperfine components began to overlap with the g_2 components and called these limits the outer edges of the middle 8-line Co multiplet. The limits were taken to be after the 7th line on the low-field side and just prior to the 4th last line or the high-field side. This analysis yielded a value of $a_2 \approx 41$ G and $g_2 \approx 2.022$.

Most important is the observation of *very little anisotropy* in the Co hfs. $a_1^{Co} - a_3^{Co}$ was about 5 G, contrasted to about 100 G for radicals like the (cyclopentadienone)cyclopentadienylcobalt anion.[13] This means that there is very *little Co d-orbital character* in the half-filled orbital. The cobalt isotropic splitting of ca. 43 G (average of a_1, a_2, and a_3, assuming the same sign) may be compared with the calculated value for an unpaired electron localized in thee 4s orbital on Co: 2124 G.[18] Thus, there is about 2% 4s spin on cobalt. This could arise from spin polarization, by interaction with hydrocarbon-based $2p_z$ carbon orbitals. But an unmistakable conclusion is that the *half-filled orbital must reside predominantly on the COT portion of the molecule.*

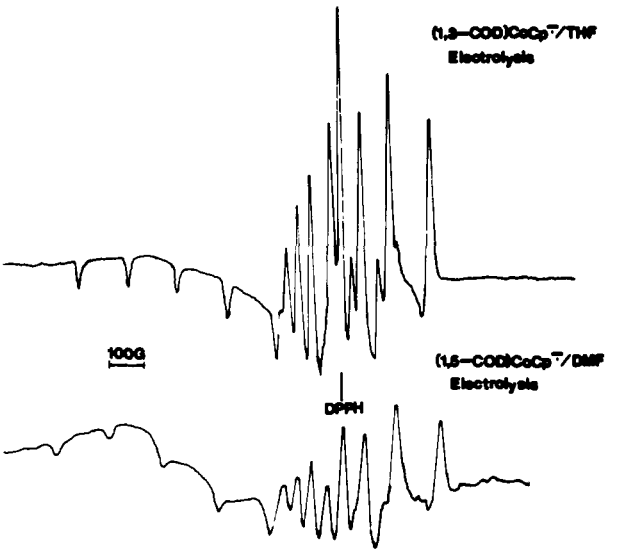

Figure 3. Frozen solution esr spectra of (1.5-COD)CoCp$^-$ (top) and (1,3-COD)CoCp$^-$ (bottom). Solutions were produced by electrolytic reduction of 10^{-3} M (1,5-COD)CoCp in DMF/0.1 M Bu_4NPF_6 (top) or in THF/0.1 M Bu_4NPF_6 (bottom) at −2.6 V at mercury pool under N_2.

(1,5-COD)CoCp$^-$ and (1,3-COD)CoCp$^-$. These anions gave spectra reminiscent of those of π-complex radicals in which the unpaired electron was cobalt based.[13,15] Since the anion of the 1,5-isomer is only stable in DMF,[1] electrolysis was performed under N_2 in this solvent at a mercury pool at −2.6 V. The solution went from light yellow to dark brown, and cyclic voltammetry scans afterward showed only the presence of the couple (1,5-COD)CoCp$^{0/-}$. A frozen solution ESR spectrum had approximately axial symmetry (Figure 3), with a_1(Co) = 158 G and $a_2 \approx a_3 \approx 50$ G.

In a THF solution isomerization of the 1,5-anion, (1,5-COD)CoCp$^-$, to that of the 1,3-anion proceeds much more rapidly.[1] Consequently, (1,3-COD)CoCp$^-$ was produced by electrolysis of the neutral compound (1,5-COD)CoCp in THF at a mercury pool at −2.6 V. A frozen solution of this sample produced an ESR spectrum (Figure 3) with approximately axial symmetry, having a_1(Co) = 140 G and $a_2 \approx a_3 \approx 42$ G. Reduction of the compound with Na/K in THF gave an identical spectrum. The anions of both isomers of the COD–Co compund were extremely seesitive to reoxidation. If the frozen samples were melted, brought briefly to room temperature, and then refrozen, the ESR signals disappeared. However, a fluid solution, isotropic, spectrum was observed for (1,3-COD)CoCp$^-$ in THF at 183 K. Even at this temperature, relaxation of the radical was very rapid, probably due to the large *g* value anisotropy, and broad lines were observed. As expected in this situation, there were large variations in the line widths of individual cobalt hyperfine lines, and several lines of the cobalt octet were too broad to measure (Figure 4). The spacings in the other lines were used to obtain the cobalt isotropic splitting, 75 G. This number is important because it is close to the average of the three values of the Co hyperfine tensor measured from the glassy spectrum, 75 G, and helps to confirm the correctness of the assignments from the frozen solution spectra.

From the observed values of the Co hyperfine tensor for both the 1,5- and 1,3-isomers of the Co–COD anions, it may be assumed

(16) Repeated attempts to generate samples for higher field (Q band) ESR analysis failed due to technical reasons associated with the air sensitivity of solutions of this ion.

(17) The values of a_2(Co) could not be calculated from a_1, a_3, and $a_{(iso)}$ because the latter was experimentally inaccessible; fluid solutions of the anion yielded no observable spectrum. This was probably due to broadening of the spectrum by rapid spin–lattice relaxation.

(18) Morton, J. R.; Preston, K. F. *J. Magn. Reson.* **1978**, *30*, 577.

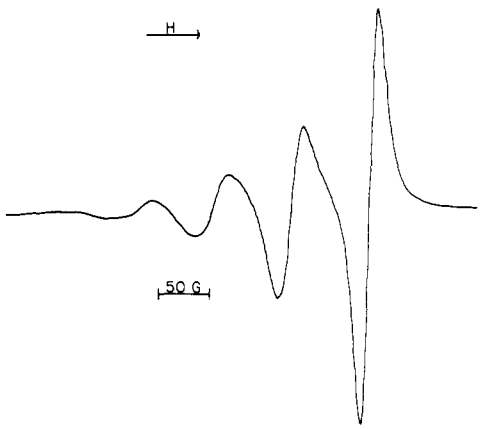

Figure 4. Isotropic, fluid solution ESR spectrum of (1,3-COD)CoCp$^-$ at 183 K. Solution was produced by electrolysis in THF as in Figure 3.

that the half-filled orbital in these species *is predominantly cobalt based*, with about 10% more metal character in the 1,5-anion than in the 1,3-anion.

Theoretical Calculations. Extended-Hückel calculations were carried out on **1**–**3** as well as **6** and **7**, serving as convenient

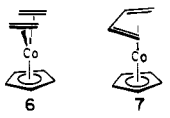

6 7

theoretical models of the cyclooctadiene complexes **4** and **5**. Geometrical and computational details aree given in the Appendix. Table II lists the composition of the lowest unoccupied molecular orbitals (LUMOs) of **1**–**3** and **6** and **7**. In agreement with our ESR data, the COT compounds have LUMOs localized mainly on the COT ligand. Furthermore, it is concentrated on the *uncomplexed* portion of the COT ring. On the other hand, the LUMOs in **6** and **7** are primarily metal based. Since our calculations neglect interelectronic repulsion terms, we should not attempt any quantitative prediction of reduction potentials. But at least between a particular pair of isomers, qualitative agreement was obtained between the relative energies of the LUMOs and the ease of reduction of the compounds. Thus, the LUMO of **2** was calculated to be ca. 0.2 eV lower in energy than that in **1**, and **2** was found to reduce at $E^\circ = -1.81$ V, and about 200 mV less negative than **1**.[7,19] Similarly, the LUMO of **7**, a model for (1,3-COD)CoCp, lies ca. 0.1 eV lower than that of **6**, a model for (1,5-COD)CoCp, and the E° value for $\mathbf{5}^{0/-}$ lies more positive than that of $\mathbf{4}^{0/-}$.[1]

A theoretical analysis of these results can be developed as follows. The important valence orbitals of a CoCp fragment are interacted with the π orbitals of a distorted COT ligand for **1** and **2**. We shall also discuss angular variations within the COT ligand and the mode of interconversion from **1** to **2**.

COT Compounds. Since the shapes and relative energies of the π orbitals of COT figure heavily into our discussion, we shall spend some time constructing them for a tub, **8**, and butadienoid, 9, geometry. The most expedient way to do this starts from the

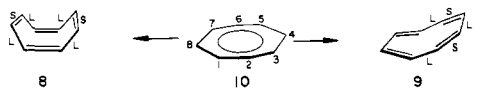

8 10 9

π orbitals of a planar COT, **10**. The relevant orbitals are shown in the middle of Figure 5. Distortion to a tub structure involves two separate motions. The first is a hinging motion bringing C_3–C_4 and C_7–C_8 up out of the plane of the other four carbons. The other motion shortens the C_3–C_4 and C_7–C_8 bonds and lengthens

(19) Note that the reduction potential reported[7] for **1**, −2.07 V, was the cathodic peak potential at a scan rate of 0.1 V/s and *not* the E° for **1**, since the reduction is irreversible. The actual E° for **1** will actually be slightly positive of the cathodic peak potential.

Table II. Percentage Composition of the LUMO[a] and Hinging Angle (θ)

compd	% ligand	% metal	% Cp (or CO)	θ, deg neutral	θ, deg anion
(1,5-COT)CoCp (1)	90	10	0	52	47
(1,3-COT)CoCp (2)	56	30	14	34	33
(1,3-COT)Fe(CO)$_3$ (3)	68	14	18	41	39
$(C_2H_4)_2$CoCp (6)	15	51	34		
(C_4H_6)CoCp (7)	20	53	27		

[a] Values of the LUMO are taken from the structure where θ was optimized for the radical anions.

C_2-C_3, C_4-C_5, etc.—as indicated by s and l in **8**. The bending motion decreases π overlap between atomic p orbitals which lie on opposite sides of the hinge. If the two orbitals are bonding with respect to each other, then that molecular level will go up in energy. Conversely, if the two orbitals are antibonding, then the molecular orbital goes down in energy. The same considerations apply in regard to bond length deformations. When both deformations act in opposite directions, the bond length deformations will tend to dominate since there is a slight gain of σ overlap which partially compensates for the loss of π overlap in the bending motions. The distortion to **8** splits the degeneracy of the e sets in **10** as shown in a somewhat exaggerated manner on the left side of Figure 5. The resusltant orbitals are labeled according to the C_{2v} symmetry of the tub structure, and only those orbitals which will heavily figure into our discussion are redrawn for **8**. There is one more point to be made concerning the evolution of the orbitals of **8** from **10**. The atomic coefficients for any π orbital in the tub structure are not the same as they were in **10**. There is an intermixing of π orbitals which have the same symmetry. For example, the lowest π orbital in planar COT and one component of e_{2u} both have a_1 symmetry in **8** and intermix upon distortion. The a_1 orbital in the middle left of Figure 5 becomes more localized on C_1, C_2, C_5, and C_6 as a consequence of this. The lower a_1 orbital, not shown in Figure 5, becomes concentrated on C_3, C_4, C_7, and C_8. More importantly, a similar perturbation occurs with the other component of e_{2u}, labeled A_2. Here mixing with the highest π level of COT localizes a_2 on C_3, C_4, C_7, and C_8. Analogous arguments can be constructed for the b_1 and b_2 combinations. The distortion of the π orbitals of planar COT to the butadienoid conformation, 9, involves folding across the C_1–C_2 and C_5–C_6 bonds. There is also a lengthening of the C_1–C_2, C_3–C_4, and C_5–C_6 bonds along with a shortening of C_2–C_3 and C_4–C_5. The energetics and shapes of the levels are traced on the right side of Figure 5. The π levels are labeled s and a depending upon whether they are symmetric or antisymmetric with respect to the mirror plane in the plane of the paper. Again considerations of the loss or gain of π bonding upon distortion to **9** can readily be constructed yielding the relative ordering of the π levels. It also can be seen that our set of distorted COT orbitals could have been developed by interacting two butadienes in the case of 9 or two sets of bisethylene fragments in **8**. One additional point worth noting about the distorted π orbitals of COT is that the component of e_{2u} which is stabilized on the butadienoid side is destabilized in the tub geometry and *vice versa* for the other component of e_{2u}. This will play an important factor when we discuss the interconversion of **1** and **2**.

An orbital interaction diagram for the construction of the orbital of (1,5-COT)CoCp (**1**) is shown in Figure 6. The valence orbitals of a CpM fragment have been extensively discussed elsewhere.[20] $1a_1$ and 1e are the remnants of an octahedral t_{2g} set. 2e and $2a_1$ are the symmetry adapted combinations of three orbitals which point to three missing ligands sites completing the octahedron. These latter three orbitals are hybridized out away from the Cp ligand and, therefore, will interact most strongly with the π orbitals

(20) Elian, M.; Chen, M. M. L.; Mingos, D. M. P.; Hoffmann, R. *Inorg. Chem.* **1976**, *15*, 1148.

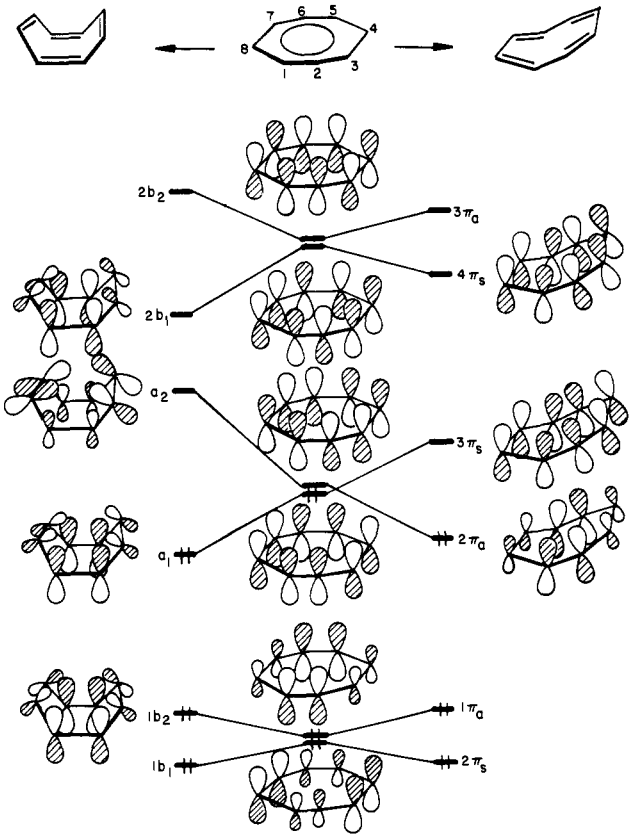

Figure 5. Development of the important π orbitals of the two distorted cyclooctatetraenes from the planar, D_{8h}, system.

of COT. The maximum symmetry for (1,5-COT)CoCp is C_s, but since the CoCp group is essentially cylindrically symmetric, the C_{2v} symmetry labels for the molecular orbitals of the molecule have been used. The 2e set on CoCp foorms strong bonding combinations with $2b_1$ and $1b_2$ of COT. One member of 1e is nonbonding, giving molecular $2a_1$. $1a_1$ andd $2a_1$ of CoCp combine with a_1 on COT to give three orbitals. Finally, the other member of 1e interacts with a_2 of COT in a bonding and antibonding fashion. The latter, shown in **11**, is found to be the LUMO of

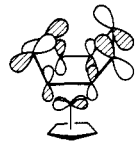

11

the molecule. The orbital resembles the fragment orbital closest to it in energy—COT a_2. In the radical anion of **1** the extra electron will reside in **11**. Recalling the polarization in COT a_2, this means that the highest electron density is actually carried by the uncomplexed portion of the COT ligand. This conclusion is not open to direct experimental test since the very limited lifetime of $\mathbf{1}^-$ has elminated detection of its ESR spectrum—$\mathbf{1}^-$ rearranges irreversibly to $\mathbf{2}^-$. However, the fact that the LUMO of **1** is $2a_2$ rather than the metal-based $2b_2$ level is essentially assured. Not only does the polarization of the π orbitals favor overlap between one member of 2e with $1b_2$ versus 1e with a_2 but also the former overlap is of a π-type while the latter is of δ symmetry. Therefore, the a_2–1e combination is not destabilized as much as the 2e–$1b_2$ one.

We have also investigated the effect of geometrical deformations on the radical anion of **1**. With the occupation of **11**, one might think that the COT ring would tend to flatten somewhat since there is bonding between C_1–C_8, C_2–C_3, C_4–C_5, and C_6–C_7. The optimized value of the hinging angle, θ, defined in **12** for **1**, was 52°. No structural data exist for directly related complexes. However, of the 1,5-COT–metal complexes which have been

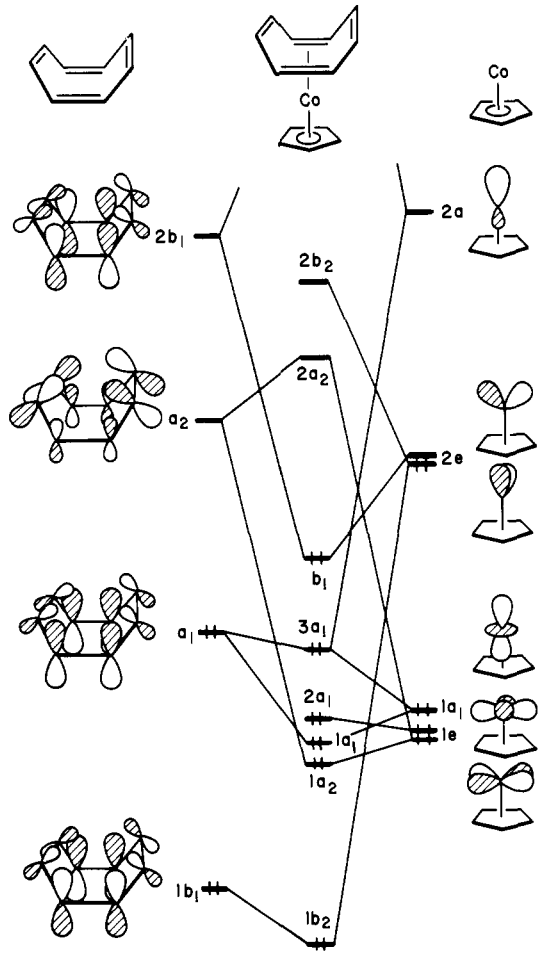

Figure 6. Orbital interaction diagram for (1.5-COT)CoCp.

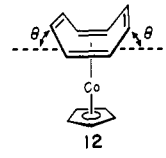

12

structurally determined,[21] values of θ from 53 to 59° have been reported. The value of θ, we calculate, diminishes a modest amount, to 47°, for the radical anion. Contraction of the C_1–C_8 etc. bonds and elongation of the C_3–C_4 and C_7–C_8 bonds along with a variation of θ does not substantially change the composition of the LUMO listed in Table II.

Figure 7 shows an orbital interaction diagram for (1,3-COT)CoCp (**2**). The 2e set of CoCp find strong bonding combinations with now $2\pi_a$ and $3\pi_s$. The other orbitals on CoCp are basically nonbonding. The important point to be noted is that the LUMO for **2** also lies at relatively low energy. It is the antibonding combination of one component of 2e with $3\pi_s$, **13**. Additionally, $4\pi_s$ mixes heavily into this orbital in a bonding fashion, **14**, which keeps the energy of the LUMO low. The resultant orbital is shown in **15**. The LUMO, 4a′ in Figure 7, then is most *heavily concentrated on the uncoordinated portion*, a smaller amount is on the metal, and very little contribution remains on the coordinated butadiene portion or Cp. The percent contribution on the metal that we calculate for **2** (see Table II) may be a little high; our ESR data suggest a smaller amount. This is perhaps due to the metal parameters used in the calculations

(21) (a) Edwards, J. D.; Howard, J. A. K.; Knox, S. A. R.; Riera, V.; Stone, F. G. A.; Woodward, P. *J. Chem. Soc., Dalton Trans.* **1976**, 75. (b) Paulus, E.; Hoppe, W.; Huber, R. *Naturwissenshaften* **1967**, *54*, 67. (c) Hill, R.; Kelly, B. A.; Kennedy, F. G.; Knox, S. A. R.; Woodward, P. *J. Chem. Soc., Chem. Commun.* **1977**, 434. (d) Baenziger, N. C.; Goebel, C. V.; Berg, T.; Doyle, J. R. *Acta Crystallogr., Sect. B* **1978**, *B34*, 1340.

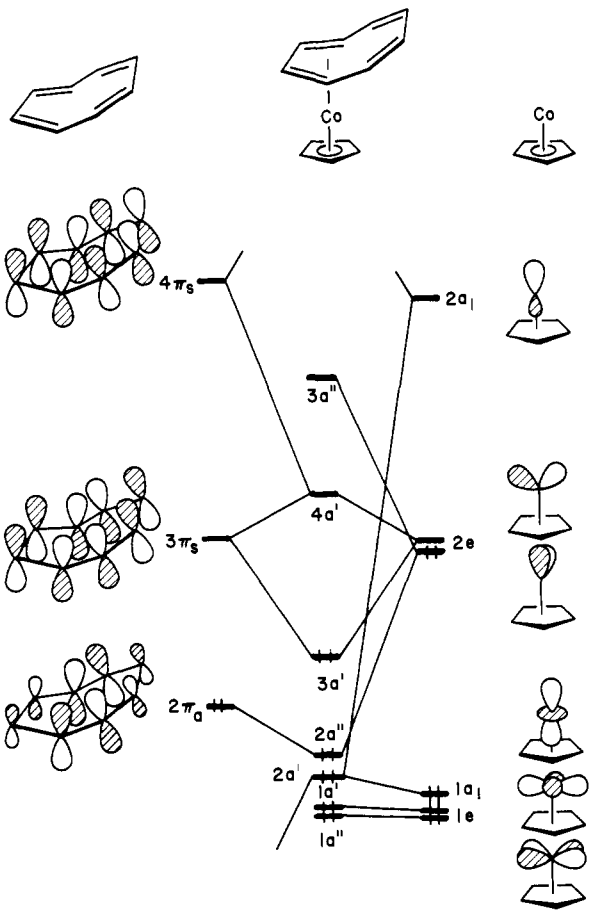

Figure 7. Orbital interaction diagram for (1,3-COT)CoCp.

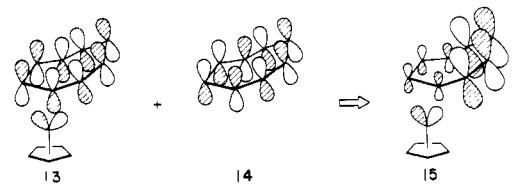

(see Appendix). The interaction diagram for building the molecular orbitals of (1,3-COT)Fe(CO)$_3$ is essentially the same as presented in Figure 7. The Fe(CO)$_3$ group is isolobal with CoCp.[20] One notices in Table II, however, that we calculate considerably less metal character in the LUMO, 4a′, of **3** compared to **2**. The reason for this lies in the energy of 2e relative to $4\pi_s$ and $3\pi_s$. As the energy of 2e goes down, its contribution in 4a′ decreases and in 3a′ increases. The one component of 2e is becoming uncoupled with $3\pi_s$ and $4\pi_s$. There still is substantial intermixing between $4\pi_s$ and $3\pi_s$ in 4a′. With our parameters the 2e set in Fe(CO)$_3$ lies 0.15 eV lower in energy thanthat in CoCp. Had we used a lower valence shell ionization potential for cobalt 3d, then the energy of the CoCp 2e would have dropped. Clearly this is a question for a more sophisticated calculational method. We have also investigated the hinging angle for the two 1,3-COT compounds, defined in **16**. As is seen in Table II the values for θ

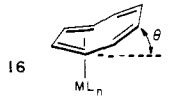

are essentially the same for the neutral species of **2** (34°) and **3** (41°) as the radical anions. Our optimized value for **3** is quite close to the experimental value of 42.5° for this compound.[22]

Perhaps the compound most closely related to **2** which has been structurally determined in η^4-1,3-COT-Ru-η^6-hexamethylbenzene.[23] Here θ was found to be 45.4°. Other complexes are in this range;[24] however, one, η^4-1,3-COT-Fe-η^6-COT,[25] has a value of θ = 33°, and η^4-1,3-COT complexes of the early transition metals[26] have values of θ from 34.4° to 21°. Therefore, our calculated value is not unreasonable. Again the percent contributions at the portions of the molecule listed in Table II for **2** and **3** do not change significantly with modest variation of θ (±10°).

As previously mentioned the LUMO for **2** is calculated to lie lower in energy than that for **1**. This outcome can conveniently be viewed in the following manner. The LUMO for **2** is essentially the LUMO of a (noncoordinated) butadiene. In **1** the LUMO is the out of phase combination of two weakly interacting ethylene π^* orbitals. The LUMO of butadiene, of course, lies at lower energy than ethylene π^*. This is an oversimplification, but it may prove heuristicly useful for other polyene-ML$_n$ complexes where the polyene is not fully coordinated to the ML$_n$ unit. However, it has been suggested[27] that in the two-electron reduction of η^6-naphthalene-Cr(CO)$_3$ complexes the extra two electrons reside on the metal and the naphthalene becomes η^4 coordinated, so some caution in extending this argument may be warranted.

Interconversion of 1 and 2. It has been shown[2,7] that the 1,3-COT and 1,5-COT isomeric forms of (COT)CoCp, **2** and **1**, are in slow equilibrium at room temperature. **1** is the thermodynamically more stable isomer in the neutral compounds. The 1,5-form has also been fouund to be the more stable one for (COT)MCp (M = Rh, Ir).[28] Equilibration of the 1,5- and 1,3-isomers of (COT)M(Me$_5$C$_5$) (M = Rh, Ir) has also been found[29] with the 1,5-isomer being thermodynamically more stable than the 1,3-one. Some effort was made to study the pathways for the interconversion of **1** and **2**. In agreement with experiment, our calculations give the 1,5-isomer **1** to be ca. 4 kcal/mol more stable than the 1,3-isomer **2**. This number is not to be taken too seriously since we have not undertaken a full geometrical optimization of both forms. In the radical anions, since the LUMO of **1** lies higher in energy than **2**, it is easy to see why **1**$^-$ irreversibly isomerizes to **2**$^-$.[1,7] We calculate **2**$^-$ to be 10 kcal/mol more stable than **1**$^-$.

There are two mirror planes to be considered in **1** for a study of the interconversion process. These are shown in **17**. The most

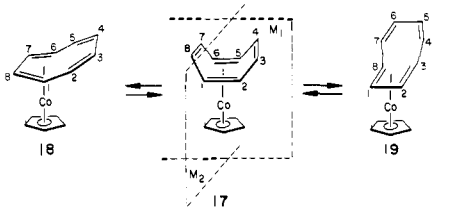

simple motion conserves the M_1 mirror plane giving **18**. Another pathway, geometrically more complicated, would conserve mirror plane M_2. Here C_5 and C_6 move up, away from cobalt and C_3 andd C_8 move down, toward it. Concomitant with this the CoCp unit must move away from the center of the COT ligand toward C_1 and C_2, giving **19**. We find that the former pathway to **18**

(22) Dickens, B.; Lipscomb, W. N. *J. Chem. Phys.* **1962**, *37*, 2084. For the PE spectra and theoretical calculations on this compound see: Böhm, M. C.; Gleiter, R. *Z. Naturforsch., B: Anorg. Chem., Org. Chem.* **1980**, *35B*, 1028.

(23) Bennett, M. A.; Matheson, T. W.; Robertson, G. B.; Smith, A. K.; Tucker, P. A. *J. Organomet. Chem.* **1976**, *121*, C18; *Inorg. Chem.* **1980**, *19*, 1014.

(24) Cotton, F. A.; Eiss, R. *J. Am. Chem. Soc.* **1969**, *91*, 6593. Bassi, I. W.; Scordamaglia, R. *J. Organomet. Chem.* **1972**, *37*, 353.

(25) Allegra, G.; Colombo, A.; Immerzi, A.; Bassi, I. W. *J. Am. Chem. Soc.*, **1968**, *90*, 4455. Allegra, G.; Colombo, A.; Mognaschi, E. R. *Gazz. Chim. Ital.* **1972**, *102*, 1060.

(26) (a) Bauer, D. J.; Krüger, C. *J. Organomet. Chem.* **1972**, *42*, 129. (b) See reference 4. (c) Bauer, D. J.; Krüger, C. *Inorg. Chem.* **1976**, *15*, 2511. (d) Cotton, F. A.; Koch, S. A. *J. Am. Chem. Soc.* **1977**, *99*, 7371. Cotton, F. A.; Koch, S. A.; Schultz, A. J.; Williams, J. M. *Inorg. Chem.* **1978**, *17*, 2093. (d) Dietrich, H.; Soltwisch, M. *Angew. Chem.* **1969**, *81*, 785.

(27) Rieke, R. D.; Arney, J. S.; Rich, W. E.; Willeford, B. R., Jr.; Poliner, B. S. *J. Am. Chem. Soc.* **1975**, *97*, 5951.

(28) Davison, A.; McFarlane, W.; Pratt, L.; Wilkinson, G. *J. Chem. Soc.* **1962**, 4821.

(29) Smith, A. K.; Maitlis, P. M. *J. Chem. Soc., Dalton Trans.* **1976**, 1773.

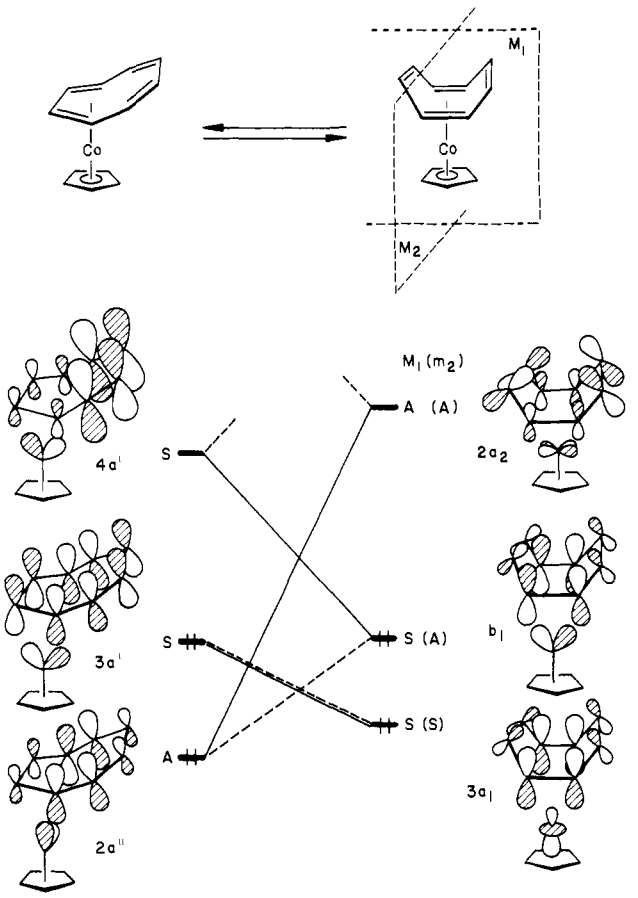

Figure 8. Partial orbital correlation diagram for the interconversion of the 1,3 (left) and 1,5 (right) isomers of (COT)CoCp. The solid line correlates orbitals where the fluxional motion conserves mirror plane M_1. The dashed line correlates those where the M_2 mirror plane is conserved.

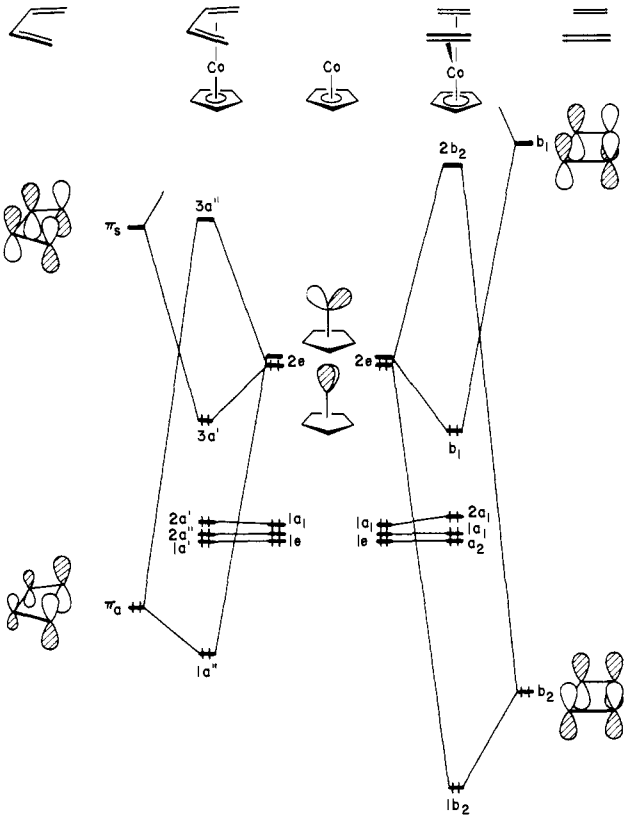

Figure 9. Interaction diagram for butadiene-CoCp (left) and bisethylene-CoCp (right).

is symmetry forbidden. The latter pathway to **19** is symmetry allowed. Figure 8 shows the evolution of the two highest lying occupied orbitals and the LUMO's for the two isomers of (COT)CoCp. Along with the symmetry labels taken from Figure 6 and 7, we have labeled the orbitals of the 1,5-isomer to be symmetric (S) or antisymmetric (A) with respect to M_1 and M_2. The corresponding three orbitals of the 1,3-isomer are shown on the left of Figure 8. They again are labeled as being symmetric or antisymmetric with respect to the mirror plane shown for the structure at the top of the figure. Conserving M_1 to **18**, one can see that the filled $3a_1$ level in **1** correlates with the filled 3a′ orbital in **2**. However, the HOMO, b_1, correlates to the LUMO, 4a′, of **2** and the LUMO, $2a_2$, goes to the filled 2a″ orbital. These correlations are shown by the solid line in Figure 8. The pathway to **18** is, therefore, symmetry forbidden[30] and is expected to require a relatively high activation energy. The second pathway which conserves M_2 is symmetry allowed. A correlation of the orbitals is given by the dashed line in Figure 8. One of the offending orbitals in **1**, b_1, is now A with respect to M_2 and will correlate with 2a″. The LUMO of **1**, $2a_2$, correlates with a higher lying, unfilled orbital. We have not calculated an activation energy for this process, but the pathway to **19** must require less energy than that to **18**. We know of no way to experimentally test this idea. Unfortunately, the (1,3-COT)CoCp isomer itself fluxional,[7] as is **3** and many other well-established analogues.[23,29,31] There are other pathways which conserve no symmetry elements that are plausbile. For example, **17** could rearrange to **20** (or any of the other three symmetry related products). An η^5 structure, **21**, or η^3, **22**, which can serve as transition states for a [1,2] shift in the 1,3-isomer[32] are also likely candidates.

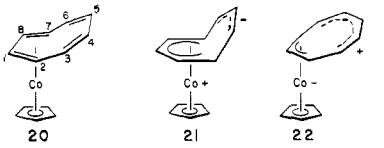

20 21 22

Cyclooctadiene Compounds. As we mentioned previously, bisethylene-CoCp (**6**) and butadiene-CoCp (**7**) serve as theoretical models for the 1,5- and 1,3-cyclooctadiene-CoCp complexes, **4** and **5**, respectively. The alkyl chains in **4** and **5** will not significantly perturb the electronic structure. The salient details of the interaction diagrams for **6** and **7** are presented in Figure 9. 1e and $1a_1$ are mainly nonbonding in both complexes. The 2e set of CoCp forms strong bonding combinations with b_2 and b_1 in **6** and π_a along with π_s in **7**. The LUMOs of **6**, $2b_2$, and **7**, 3a″, are the antibonding interactions between b_2 and π_a with 2e. The molecular orbital most closely represents that fragment orbital nearest in energy to it—a *metal*-based one. Therefore, the extra electron in the reduced species of **4** and **5** is metal centered (see Table II), in contrast to **1–3**. The two π systems in the bisethylene or 1,5-cyclooctadiene ligand only weakly interact with each other. That in the butadiene or 1,3-cyclooctadiene ligands are more strongly coupled. This sends π_a to higher energy than b_2 and π_s drops in energy with respect to b_1. Accordingly, the energy difference between π_a and 2e will be less than that between b_2 and 2e. One expects from a perturbation theory argument that 3a″, 1a″ will be split in energy greater than $1b_2$, $2b_2$, which immediately leads to the LUMO of **6** lying lower than that in **7**. In actual fact the reverse is found from our calculations on **6** and **7**. Furthermore, **5** is more easily reduced than **4**. The explanation for this lies in an overlap difference of π_a and b_2 with 2e. The

(30) A full analysis shows that in **1** there are 23 occupied orbitals (excluding core electrons) S with respect to M_1 and 14 of the A type. In **2** there are 22 occupied S orbitals and 15 of A symmetry. On the other hand in **1** there are for mirror plane M_2, 22 occupied S and 15 occupied A levels.

(31) Cotton, F. A.; Davison, A.; Marks, T. J.; Musco, A. *J. Am. Chem. Soc.* **1969**, *91*, 6598. Cotton, F. A.; Hunter, D. L. *Ibid.* **1976**, *98*, 1413, see ref 3 for a full listing.

(32) Dedieu, A.; Hoffmann, R., to be submitted for publication.

Table III. Parameters Used in the Extended-Hückel Calculations

orbital	H_{ij}, eV	ζ_1	ζ_2[a]	C_1[a]	C_2[a]
Fe 3d	−12.70	5.35	1.80	0.5366	0.6678
4s	−9.17	1.90			
4p	−5.37	1.90			
Co 3d	−12.11	5.55	2.10	0.5680	0.6060
4s	−8.54	2.00			
4p	−4.76	2.00			
C 2s	−21.40	1.625			
2p	−11.40	1.625			
O 2s	−32.30	2.275			
2p	−14.80	2.275			
H 1a	−13.60	1.30			

[a] Contraction coefficients used in the double-ζ expansion.

value for the former (0.203) is larger than that for the latter (0.165). In the bisethylene (as well as 1,5-cyclooctadiene) complex, the π face of the ethylenes rotates so that they point toward the metal; see **23**. This maximizes the overlap between the π

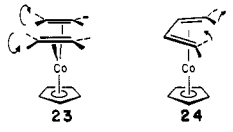

23 **24**

orbitals and 2e. On the other hand, the two interior hydrogens (or alkyl chains for **5**) in the butadiene complex are likely, in comparison with other butadiene structures, to move up, out of the plane, as in **24**. Therefore, the π system in **24** cannot fully reorient itself as well as that in **23**. To reiterate, it is the greater overlap in **4** that makes the complex more difficult than **5** to reduce rather than energy gap argument between the fragment orbitals.

Conclusions

The experimental work and calculations present a consistent picture of the LUMO orbitals involved in the reduction of these cycloocta-ene metal compounds. Reduction of the cyclooctatetraene compounds **1**, **2**, or **3** occurs via addition of an electron to an orbital which is based largely on the COT portion of the molecule. In the formal sense, then, the anions (1,5-COT)CoCp$^-$ and (1,3-COT)CoCp$^-$ remain Co(I) species. One of the most interesting results of the calculations is that the unpaired electron resides on the 4-carbon COT fragment which is *not complexed* to the metal. It makes sense, then, that for (1,5-COD)CoCp and (1,3 COD)CoCp, in which the uncomplexed uncomplexes carbons cannot accept the extra electron (i.e., they are already saturated), the reduction occurs into a metal-based orbital, making the formal metal oxidation state in (1,5-COD)CoCp$^-$ and (1,3 COD)COCp$^-$ Co(0).

Acknowledgment. The work at University of Vermont was supported by the National Science Foundation, Grants CHE 76-83668 and CHE 80-04242; that at University of Houston was supported by the Robert A. Welch Foundation and the Scientific Affairs Division of NATO. T.A.A. thanks the hospitality of Professor Peter Hofmann at University of Erlangen where some of the work was carried out and Professor Ray Davis for unpublished information.

Appendix

The parameters used in the extended-Hückel calculations are listed in Table III. The H_{ij}'s for iron and cobalt were obtained from charge iterative calculations on butadiene-Fe(CO)$_3$ and π-allyl-Co(CO)$_3$.[33] A modified scheme for the computation of H_{ij}'s was used.[34] The Co–Cp distance used for all complexes was set at 1.687 Å, and all C–C and C–H distances were put at 1.41 and 1.09 Å, respectively, unless otherwise noted. In **1** the Co–COT distance was set at 1.40 Å. The C_2–C_3 etc. and C_3–C_4 etc. distances were fixed at 1.45 and 1.34 Å, respectively. The geometrical parameters in **6** were modelled after those in **1**. The geometry of **3** was set at that for the observed structure,[22] and the geometrical parameters in **2** were also given these values. The Fe–C and C–O distances in **3** were idealized at 1.78 and 1.14 Å, respectively. The (O)C–Fe–C(O) angles were set at 90°.

(33) Albright, T. A.; Hofmann, P.; Hoffmann, R. *J. Am. Chem. Soc.* **1977**, *99*, 7546.
(34) Ammeter, J. H.; Bürgi, H. B.; Thibeault, J. C.; Hoffmann, R. *J. Am. Chem. Soc.* **1978**, *100*, 3686.